

# Capillary rise method for the measurement of the contact angle of soils

Zhen Liu · Xiong Yu · Lin Wan

Received: 17 November 2013 / Accepted: 27 August 2014  
© Springer-Verlag Berlin Heidelberg 2014

**Abstract** The contact angle quantitatively describes the contact on the liquid–solid interface and is thus critical to many physical processes involving interactions between soils and water. However, the role of the contact angle in soils is far from being adequately recognized. This paper reports a comprehensive study on the application of the capillary rise method (CRM) to measure the contact angles of soils. The deviations of analytical solutions to various forms of the Lucas–Washburn equation were presented to offer a detailed study on the theoretical basis for applying CRM to soils, which is absent in existing studies. The disadvantages of the conventional CRM investigations were demonstrated with experiments. Based on a comparative study, a modified CRM was proposed based on the analytical solution to one form of the Lucas–Washburn equation. This modified CRM exhibited a reliable performance on numerous unsieved and sieved (different average particle sizes) specimens made of a subgrade soil and a silicon dioxide sand. Procedures for the specimen

preparation were designed and strictly followed, and innovative apparatuses for the preparation, transport, and accommodation of soil specimens were fabricated to ensure repeatability. For the modified CRM, experimental results for unsieved specimens exhibited good repeatability, while for sieved soils, clear trends were observed in the variations of the contact angle with particle size. Contact angles much greater than zero were observed for all of the tested soil specimens. The results indicate that the assumption of perfect wettability, which is adopted in many existing geotechnical studies involving the contact angle, is unrealistic.

**Keywords** Capillary rise method · Contact angle · Lucas–Washburn equation · Soil water characteristic curve

## 1 Introduction

The contact angle, or more specifically, the angle between liquid–gas and liquid–solid interfaces, is an intrinsic property of solid–liquid–gas systems such as soils [36]. It is of great significance in many soil physical processes involving the interaction between soil and water [3, 14]. For example, it is critical to water infiltration, redistribution, groundwater recharge, solute transport in unsaturated zones, compaction and aeration in variably saturated soils, and temperature-induced water redistribution [5, 24]. This is because this property quantifies the ability of a liquid to spread on another solid [32]. Taking the soil water characteristic curve (SWCC) for example, this key relationship in unsaturated soil mechanics depends on both the soil matrix tomography (i.e., pore-size distribution) and surface physical chemistry (i.e., contact angle). While the pore-size distribution has been extensively studied for SWCCs, the

---

Z. Liu  
Department of Civil Engineering and Environmental  
Engineering, Michigan Technological University,  
1400 Townsend Drive, Dillman 201F, Houghton,  
MI 49931, USA  
e-mail: zhenl@mtu.edu

X. Yu (✉)  
Department of Civil Engineering, Case Western Reserve  
University, 10900 Euclid Avenue, Bingham 206, Cleveland,  
OH 44106-7201, USA  
e-mail: xxy21@case.edu

L. Wan  
Department of Civil Engineering, Case Western Reserve  
University, 10900 Euclid Avenue, Bingham 259, Cleveland,  
OH 44106-7201, USA  
e-mail: lin.wan@case.edu

contact angle is usually assumed to be a constant, mostly zero, for simplicity in view of the high surface energy of soil minerals [4, 5, 18]. However, despite a few investigations into the effect of the contact angle [34], these assumptions of a constant (or zero) contact angle corresponding to an invariant (or perfect) wettability, especially in a wetting process, have rarely been validated by experimental evidence. In fact, a varying contact angle value (nonzero) with respect to various factors, such as water potential, roughness, and temperature, has been frequently reported by the outsiders of geotechnical engineering, such as soil scientists, agricultural engineers, and physical chemists [15, 22, 23, 46, 47].

Various methods have been proposed for the measurement of the contact angles of soils on the basis of different mechanisms, e.g., the water drop penetration time [13, 31, 40], the molarity of an ethanol droplet [12, 28], and the flotation time [43, 49]. More recently, the CRM [2], the sessile drop method [6] and Wilhelmy plate method [7] have been developed for soils. Among these methods, the CRM based on the Lucas–Washburn equation [38, 59] is by nature suitable for hydrophilic soils, which exactly cover the soils affiliated with SWCCs in geotechnical engineering. One distinct advantage of this method is that it is capable of assessing the average contact angle of a bulk of soil rather than that of several layers of the soil close to the surface. This average contact angle which is essentially the average apparent contact angle is different from the intrinsic contact angle between water and a flat smooth mineral interface. Instead, it represents the average contact angle of a conceptualized bundle of cylindrical capillaries (BCC) [57], which is also the conceptual model used by most SWCC formulations. Therefore, the CRM is by nature suitable for porous materials such as soils.

Despite the development of the Lucas–Washburn equation since 1920s [38, 59], the CRM for porous materials based on this equation had not been extensively investigated until 1990s [2]. Due to this reason, there are only a few attempts at applying this type of method to soils. The earliest effort was the study of Letey et al. [32] on the measurement of liquid–solid contact angles in soils based on both Poiseuille’s approximation and the force balance for infiltration into soil, which were equivalent to the Lucas–Washburn equation. Siebold et al. [53] applied the CRM to silica flour and calcium carbonate by measuring both the height (by a scale) and mass (by Kruss 12 tensiometer) of imbibed liquids. Michel et al. [41] measured the wettability of partly decomposed peats with a Kruss 12 tensiometer based on the CRM, in which the tortuosity of the capillaries was considered. Abu-Zreig et al. [1] made a

simple application of the CRM for measuring the contact angles between soils and various test liquids while studying the effect of surfactants on hydraulic properties of soils. Geobel et al. [22] claimed their study to be the first one that applied the CRM to soil aggregates. In this study, the masses of imbibed liquids were measured with an electronic balance, and details in experiment setup and influencing factors were discussed. Ramirez-Flores et al. [47] followed Goebel’s method [22] for measuring the contact angles of intact soil aggregates, packing of intact aggregates, and packing of crushed aggregates of nine topsoils and three humus subsoils.

A recent publication of the authors [35] reported that the contact angle may play a significant role in unsaturated soils via the SWCC. And a modified way for implementing CRM was briefly introduced, but not detailed. This study presents a comprehensive study for applying the CRM to the contact angle measurement of hydrophilic soils. The deviations of analytical solutions to various forms of the Lucas–Washburn equation were presented to offer a detailed study on the theoretical basis for applying the CRM to soils, which is absent in existing studies. Measures were taken to overcome several difficulties, preventing accurate contact angle measurements with the CRM: (1) a self-fabricated tube with special design to eliminate external meniscus; (2) specially designed soil specimen preparation procedures to ensure consistency in sample qualities and repeatability of experiments; and (3) automatic data processing to avoid subjective factors. A comparative study is conducted to evaluate several different ways for implementing the CRM, which includes the one used by most of the existing studies. A modified CRM method is suggested and validated based on the comparative study. Contact angles were measured for the specimens made of two typical soils, either sieved or unsieved. This pioneering study will provide a complete and detailed reference for later investigations into the contact angle of soils, especially those using the CRM, which are expected to be boomed as the significant role of the contact angle is more and more clearly realized.

## 2 Theory

There are four types of forces involved in the dynamic process of a capillary rise in a cylindrical tube or a capillary. These forces include surface tension, inertial force, viscous force, and gravity. Thus, the governing equation is obtained by ensuring the equilibrium of imbibed water by allowing for these forces (Eq. 1) [27, 62].

$$\underbrace{2\pi r \gamma \cos(\theta)}_{\text{Surface Tension}} - \underbrace{\rho \pi r^2 \frac{\partial}{\partial t} \left[ h(t) \frac{\partial h(t)}{\partial t} \right]}_{\text{Inertial Force}} - \underbrace{8\pi \eta h(t) \frac{\partial h(t)}{\partial t}}_{\text{Viscous Force}} - \underbrace{\rho \pi r^2 g h(t)}_{\text{Gravity}} = 0 \quad (1)$$

where the four terms on the left-hand side represent surface tension, inertial force, viscous force and gravity, respectively;  $r$  is the radius of the tube;  $\gamma$  is the surface tension of the interface between the test (imbibed) liquid and gas;  $\theta$  is the contact angle;  $t$  is time;  $h(t)$  is the height of the capillary rise at time  $t$ ;  $\eta$  and  $\rho$  are the dynamic viscosity and density of the test liquid, respectively; and  $g$  is the gravitational acceleration. The positive or negative sign in front of a term indicates the corresponding force is a motivation or a resistance to the capillary rise. This equation was developed based on the following assumptions [19]. (1) The flow is one-dimensional. (2) There is no friction or inertia effect caused by displaced air. (3) There is no inertia or entry effect in the liquid reservoir. (4) The viscous pressure loss inside the tube is given by the Hagen–Poiseuille law. Equation 1 strictly describes the variation of the capillary height with time once all the assumptions are ensured. This equation can be simplified as Eq. 2.

$$B - A(hh')' - Chh' - Dh = 0 \quad (2)$$

where  $A = \rho \pi r^2$ ;  $B = 2\pi r \gamma \cos(\theta)$ ;  $C = 8\pi \eta$ ; and  $D = \rho \pi r^2 g$ .

Equation 1 is the most up-to-date form of the Lucas–Washburn equation based on modifications to the original ones with and without gravity [51]. The Lucas–Washburn equation was designated to describe the dynamics of a capillary rise in a single cylindrical capillary or tube. When extending this equation to porous materials such as soils, the porous medium is conceptualized as a BCC. This conceptual model of a BCC of different radii has also been frequently used in unsaturated soil mechanics for the development of SWCCs. For the dynamics of the capillary rise, the original BCC of different radii was then equivalently viewed as another bundle of capillaries of an identical radius [33]. This radius is called the effective radius (or average radius). The Lucas–Washburn equation is assumed to be valid for the capillary rise in every capillary within the equivalent bundle.

There is a unique solution to the above ordinary differential equation (ODE) once the porous material ( $r$ ) and test liquid ( $\rho, \eta$ ) are determined ( $\theta$  is dependent on both the porous material and the test liquid). But unfortunately, there is no analytical solution available for the above ODE. And our preliminary study indicated that direct curve fitting with the above ODE to experimental data requires a

capacity of optimization that is far beyond what is currently available. So, in the current stage, a feasible strategy is to obtain an analytical solution to a simplified form of the above complete Lucas–Washburn equation and then to perform curve fitting with the analytical solution to the simplified form. This is actually the strategy used by the aforementioned CRM studies. Depending on the simplifications employed, four methods for implementing the CRM can be obtained, which will be introduced in the following subsections.

### 2.1 CRM without gravity and inertia (method 1)

The influences of inertia and gravity were neglected in most of the existing CRM studies. Consequently, a simplified Lucas–Washburn equation which is familiar to researchers can be obtained in the following form.

$$\underbrace{2\pi r \gamma \cos(\theta)}_{\text{Surface Tension}} - \underbrace{8\pi \eta h(t) \frac{\partial h(t)}{\partial t}}_{\text{Viscous Force}} = 0 \quad (B - Chh' = 0) \quad (3)$$

The analytical solution to this simplified Lucas–Washburn equation predicts a linear relationship between the squared height of imbibed liquid and time [2, 59]. This analytical solution can then be used for curve fitting to compute the contact angle.

$$h = \left( \frac{2B}{C} t \right)^{1/2} = \left( \frac{r \gamma \cos \theta}{2\eta} t \right)^{1/2} \quad (4)$$

It is possible that the height of the liquid front is not visible or that the liquid front does not accurately reflect the inner progression of the liquid in the porous material. Hence, the above solution (height gain) is reformatted into the form of imbibed mass (mass gain). An equivalent equation was then obtained, which was used by most CRM studies [53]. Here we formulate the equation in the following way to be consistent with the BCC theory.

$$m = \left( \pi^2 r^5 N \cdot \frac{\rho^2 \gamma}{2\eta} \cdot \cos \theta \cdot t \right)^{1/2} \quad (5)$$

where  $N$  is the number of equivalent capillaries in a capillary rise process, and  $\pi^2 r^5 N$  is usually referred to as Washburn constant. Stange [54] and Fries and Dreyer [20] believed that the very first stage was purely dominated by inertial forces, and subsequently the influence of viscosity increases (visco-inertial flow). After that, the effect of inertia vanishes and the flow becomes purely viscous. This viscosity-dominant period corresponds to a mechanism described by Eqs. 3–5. But the influence of gravity has been proven to be significant when height of the capillary reaches one-tenth of the equilibrium height [20]. So the application of this method requires identifying a stage

when the above equation can satisfactorily describe the dynamics of the capillary rise. However, it is possible that such a stage is very short or even does not evidently exist. Even if there exists such a stage, a segment of the  $m^2$ - $t$  curve whose tangent has the least slope variation needs to be identified for a subsequent linear regression to determine the contact angle [53]. Thus, the implementation of the method could be very subjective. These two concerns were investigated by experiments and will be introduced later in this study.

## 2.2 CRM without gravity (method 2)

As mentioned, no explicit solution to the complete Lucas–Washburn equation is available by now. Nonetheless, the simplified Washburn equation used by Method 1 can still be improved by taking into account the inertial force. This consequent equation (Eq. 6) is possibly able to provide a good prediction for the capillary rise, especially when the height of water front is much less than the equilibrium height.

$$\underbrace{2\pi r\gamma \cos(\theta)}_{\text{Surface Tension}} - \underbrace{\rho\pi r^2 \frac{\partial}{\partial t} \left[ h(t) \frac{\partial h(t)}{\partial t} \right]}_{\text{Inertial Force}} - \underbrace{8\pi\eta h(t) \frac{\partial h(t)}{\partial t}}_{\text{Viscous Force}} = 0$$

$$(B - A(hh')' - Chh' = 0) \quad (6)$$

An explicit analytical solution to the above equation is possible and can be formulated as Eq. 7.

$$h = \left[ \frac{C_1}{A} - \frac{C_1}{A} \exp\left(-\frac{C}{A}t\right) + \frac{2B}{C}t \right]^{1/2}$$

$$= \left[ \frac{C_1}{\rho\pi r^2} - \frac{C_1}{\rho\pi r^2} \exp\left(-\frac{8\eta}{\rho r^2}t\right) + \frac{r\gamma \cos \theta}{2\eta}t \right]^{1/2} \quad (7)$$

where  $C_1$  is a constant. The solution could be reformatted to describe the variation of mass as Eq. 8.

$$m = \left[ C_1\rho\pi r^2 N - C_1\rho\pi r^2 N \exp\left(-\frac{8\eta}{\rho r^2}t\right) + \pi^2 r^5 N \cdot \frac{\rho^2 \gamma}{2\eta} \cdot \cos \theta \cdot t \right]^{1/2} \quad (8)$$

It is the first time an analytical solution to this form of Lucas–Washburn equation is obtained. Therefore, this solution has never been used in previous CRM studies. Its application to CRM was also tested by experiments in this study.

## 2.3 CRM without inertia (method 3)

Alternatively, the influence of gravity instead of inertia could be considered as Eq. 9. This equation is valid as long as the effect of inertia is negligible.

$$\underbrace{2\pi r\gamma \cos(\theta)}_{\text{Surface Tension}} - \underbrace{8\pi\eta h(t) \frac{\partial h(t)}{\partial t}}_{\text{Viscous Force}} - \underbrace{\rho\pi r^2 g h(t)}_{\text{Gravity}} = 0$$

$$(B - Chh' - Dh = 0) \quad (9)$$

The analytical solution could be obtained using MATLAB.

$$h = \frac{B}{D} \left\{ 1 - \frac{1}{\exp[\omega(-1 - \frac{D^2}{BC}t)] \exp(1 + \frac{D^2}{BC}t)} \right\} \quad (10)$$

where  $\omega$  represents the Wright Omega function. This equation can be further reduced to Eq. 11. Fries and Dreyer [19] obtained a similar equation in a different way.

$$h = \frac{B}{D} \left\{ 1 - W \left[ \exp\left(-1 - \frac{D^2}{BC}t\right) \right] \right\} \quad (11)$$

where  $W$  is the Lambert W function. That is,

$$h = \frac{2\gamma \cos(\theta)}{\rho g r} \left\{ 1 - W \left[ \exp\left(-1 - \frac{\rho^2 g^2 r^3}{16\gamma\eta \cos(\theta)}t\right) \right] \right\} \quad (12)$$

The solution is reformatted to describe the variation of mass.

$$m = \frac{2\pi r N \gamma \cos(\theta)}{g} \left\{ 1 - W \left[ \exp\left(-1 - \frac{\rho^2 g^2 r^3}{16\gamma\eta \cos(\theta)}t\right) \right] \right\} \quad (13)$$

The Lambert W function cannot be expressed in terms of elementary functions. The piecewise equation proposed by Barry et al. [8] was used to approximate this equation in this study. An alternative is to use the Taylor series of the above equation around 0 based on the Lagrange inversion theorem as follows,

$$m = \frac{2\pi r N \gamma \cos(\theta)}{g} \left\{ 1 - \sum_{n=0}^{\infty} \left[ \frac{(-n-1)^n}{(n+1)!} \times \frac{1}{e^n} \exp\left(-\frac{\rho^2 g^2 r^3}{16\gamma\eta \cos(\theta)}nt\right) \right] \right\} \quad (14)$$

where  $e$  is the base of natural logarithm.

## 2.4 Application to porous materials

Czachor [10] claimed that two features of porous materials should be responsible for the overestimations of the contact angle by applying the Lucas–Washburn equation to porous materials: cross section and tortuosity. But according to the definition of the apparent contact angle of porous materials

[25, 42], the intergranular characteristic has already been taken into account. The contact angle of a porous medium measured with the CRM is the apparent contact angle considering roughness. The effects of the roughness of internal pores on the difference between the apparent contact angle and intrinsic contact angle (Young's contact angle) have been extensively discussed [9, 15, 30, 46, 48, 50, 55]. However, tortuosity was not included in the definition of the apparent contact angle. As the result, the influence of tortuosity on the applications of the CRM based on the Lucas–Washburn equation to measure the apparent contact angle of porous materials deserves close attention. According to Czachor [11], the tortuosity  $\tau$  is defined as the ratio of the actual path taken by a moving liquid through pores,  $\tilde{h}$ , and the distance between the start and final heights,  $h$  [17, 52, 58].

$$\tilde{h} = \tau h \quad (15)$$

The Lucas–Washburn equation taking into account tortuosity of the porous material is as Eq. 16.

$$\underbrace{2\pi\tilde{r}\gamma\cos(\tilde{\theta})}_{\text{Surface Tension}} - \underbrace{\rho\pi\tilde{r}^2\frac{\partial}{\partial t}\left[\tilde{h}(t)\frac{\partial\tilde{h}(t)}{\partial t}\right]}_{\text{Inertial Force}} - \underbrace{8\pi\eta\tilde{h}(t)\frac{\partial\tilde{h}(t)}{\partial t}}_{\text{Viscous Force}} - \underbrace{\rho\pi\tilde{r}^2g\tilde{h}(t)}_{\text{Gravity}} = 0 \quad (16)$$

where  $\tilde{r}$  and  $\tilde{\theta}$  are the effective pore radius and the contact angle considering tortuosity, respectively. Their values may differ from those obtained by fitting experimental data with the original Lucas–Washburn equation. Equation 16 needs to be transformed in terms of the apparent rise of capillary instead of the actual path as Eq. 17 to take advantage of measured data.

$$\underbrace{2\pi\tilde{r}\gamma\cos(\tilde{\theta})}_{\text{Surface Tension}} - \underbrace{\rho\pi\tilde{r}^2\tau^2\frac{\partial}{\partial t}\left[h(t)\frac{\partial h(t)}{\partial t}\right]}_{\text{Inertial Force}} - \underbrace{8\pi\eta\tau^2h(t)\frac{\partial h(t)}{\partial t}}_{\text{Viscous Force}} - \underbrace{\rho\pi\tilde{r}^2g\tau h(t)}_{\text{Gravity}} = 0 \quad (17)$$

Equation 17 can be simplified as Eq. 18.

$$\tilde{B} - \tilde{A}(hh')' - \tilde{C}hh' - \tilde{D}h = 0 \quad (18)$$

where  $\tilde{A} = \rho\pi\tilde{r}^2\tau^2$ ,  $\tilde{B} = 2\pi\tilde{r}\gamma\cos(\tilde{\theta})$ ,  $\tilde{C} = 8\pi\eta\tau^2$ , and  $\tilde{D} = \rho\pi\tilde{r}^2g\tau$ . In fact, the values of  $\tilde{A}$ ,  $\tilde{B}$ ,  $\tilde{C}$  and  $\tilde{D}$  are equal to those of  $A$ ,  $B$ ,  $C$  and  $D$ , respectively, from curve fitting, but here we use different notations to indicate the different physical meanings.

Based on the above discussion, it is clear that the fitting functions derived in 2.1, 2.2 and 2.3 need to be adjusted to allow for tortuosity prior to applications. The adjusted governing equations (ODEs), fitting functions, and desired

fitting constants containing the contact angle for height gain and mass gain, respectively, are summarized in Table 1. The fitting functions were summarized in the following way to achieve a unified framework to integrate and compare the different models that are currently available. The fitting constant,  $\kappa_J$  ( $J = 1, 2, 3$ ), was chosen because it contains all the unknowns, and also because, in such a way this study could be consistent with the existing CRM studies.

Gurau and Mann [26] proposed a fitting function for using the CRM to characterize the wettability of gas diffusion media for proton exchange membrane in fuel cells. This equation, which is an extension to Method 1 by allowing for the influence of the external meniscus and the mass absorbed on the balance before measurements, yielded satisfactory results in their study. This fitting equation was evaluated as Method 4 in the comparative study introduced later.

$$m = m_0 + \alpha_4 \tanh(\beta_4 t) + (\kappa_4 t)^{1/2} \quad (\text{Method 4}) \quad (19)$$

where  $m_0$  is the mass absorbed on the balance, and the second term was used to describe the mass increase caused by the external meniscus. A term similar to  $m_0$  was added to the fitting functions of Methods 1, 2, and 3 in the following analyses.

### 3 Materials and method

#### 3.1 Method

Table 1 summarizes three fitting equations based on the Lucas–Washburn equation including the simplified one (Method 1) used by most existing studies for applying the CRM in soils. Together with Method 4, these fitting equations are adopted to fit measured  $m-t$  relationships when using the CRM to measure apparent contact angles of soils. For this purpose, constants in the fitting equations, i.e.,  $A$ ,  $B$ ,  $C$ ,  $D$ , or their combinations such as  $\kappa_J$  ( $J = 1, 2, 3$  and 4) will be determined. Based on these constants, there are two ways to obtain contact angles. One approach is for height gain fitting functions only. Because the effective radius and apparent contact angle are the two unknowns, the apparent contact angle can be calculated with an additional relationship between the effective radius and the contact angle [61]. But more often, water and another test liquid for reference are used for the second approach. The employment of a reference liquid is necessary for the weight gain fitting functions due to the existence of three unknowns. The reference liquid is usually an organic solvent with low surface energy, such as hexane and pentane. Pentane was used in this study. Considering the comparatively high surface energy of soil particles and low surface tension of the test liquid, the contact angle between the test liquid and soils is approximately zero.

**Table 1** ODEs, fitting functions and constants containing the contact angle for different methods

Method	Method 1 (2.1)	Method 2 (2.2)	Method 3 (2.3)
ODE	$h = \left(\frac{2\tilde{B}}{\tilde{C}}t\right)^{1/2}$	$h = \left[\frac{C_1}{\tilde{A}} - \frac{C_1}{\tilde{A}} \exp\left(-\frac{\tilde{C}}{\tilde{A}}t\right) + \frac{2\tilde{B}}{\tilde{C}}t\right]^{1/2}$	$h = \frac{\tilde{B}}{\tilde{D}} \left\{1 - W\left[\exp\left(-1 - \frac{\tilde{D}^2}{\tilde{B}\tilde{C}}t\right)\right]\right\}$
Function	$h = (\kappa_1 t)^{1/2}$	$h = [\alpha_2 - \alpha_2 \exp(-\beta_2 t) + \kappa_2 t]^{1/2}$	$h = \kappa_3 \{1 - W[\exp(-1 - \alpha_3 t)]\}$
Constant	$\kappa_1 = \frac{2\tilde{B}}{\tilde{C}} = \frac{\tilde{r}\gamma \cos(\tilde{\theta})}{2\eta\tilde{r}^2}$	$\kappa_2 = \frac{2\tilde{B}}{\tilde{C}} = \frac{\tilde{r}\gamma \cos(\tilde{\theta})}{2\eta\tilde{r}^2}$	$\kappa_3 = \frac{\tilde{B}}{\tilde{D}} = \frac{2\gamma \cos(\tilde{\theta})}{\rho g \tilde{r}^2}$
ODE	$m = \tilde{M} \left(\frac{2\tilde{B}}{\tilde{C}}t\right)^{1/2}$	$m = \tilde{M} \left[\frac{C_1}{\tilde{A}} - \frac{C_1}{\tilde{A}} \exp\left(-\frac{\tilde{C}}{\tilde{A}}t\right) + \frac{2\tilde{B}}{\tilde{C}}t\right]^{1/2}$	$m = \frac{\tilde{B}\tilde{M}}{\tilde{D}} \left\{1 - W\left[\exp\left(-1 - \frac{\tilde{D}^2}{\tilde{B}\tilde{C}}t\right)\right]\right\}$
Function	$m = (\kappa_1 t)^{1/2}$	$m = [\alpha_2 - \alpha_2 \exp(-\beta_2 t) + \kappa_2 t]^{1/2}$	$m = \kappa_3 \{1 - W[\exp(-1 - \alpha_3 t)]\}$
Constant	$\kappa_1 = \frac{2\tilde{B}\tilde{M}^2}{\tilde{C}} = \frac{\rho^2 \pi^2 \tilde{r}^5 \gamma N^2 \cos(\tilde{\theta})}{2\eta\tilde{r}^2}$	$\kappa_2 = \frac{2\tilde{B}\tilde{M}^2}{\tilde{C}} = \frac{\rho^2 \pi^2 \tilde{r}^5 \gamma N^2 \cos(\tilde{\theta})}{2\eta\tilde{r}^2}$	$\kappa_3 = \frac{\tilde{B}\tilde{M}}{\tilde{D}} = \frac{2\pi\tilde{r}\gamma N \cos(\tilde{\theta})}{g\tau}$

$\tilde{M} = \rho\pi\tilde{r}^2N$ ;  $\alpha$ ,  $\beta$ ,  $\kappa$  are the combinations of the basic fitting constants, i.e.,  $\tilde{A}$ ,  $\tilde{B}$ ,  $\tilde{C}$  and  $\tilde{D}$

With two  $\kappa_J$ 's ( $\kappa_{J,w}$  and  $\kappa_{J,p}$ ) obtained by water and the reference liquid, the apparent contact angle between water and soils can be calculated using the following equations for different methods:

$$\theta_J = \arccos\left(\frac{\kappa_{J,w}}{\kappa_{J,p}} \cdot \frac{\eta_w \rho_p^2 \gamma_p}{\eta_p \rho_w^2 \gamma_w}\right), \quad (J = 1, 2, 4) \quad (20)$$

$$\theta_3 = \arccos\left(\frac{\kappa_{3,w}}{\kappa_{3,p}} \cdot \frac{\gamma_p}{\gamma_w}\right) \quad (21)$$

where  $\theta_J$  is the contact angle obtained by Method  $J$ ;  $\kappa_{J,p}$  and  $\kappa_{J,w}$  are the constants pertaining to pentane and water, respectively, by using Method  $J$ ;  $\rho_p$  and  $\gamma_p$  are the density and surface tension of pentane, respectively;  $\rho_w$  and  $\gamma_w$  are the density and surface tension of water, respectively. Other parameters relevant to the properties of soils such as the effective radius and number of capillaries were canceled out. It is worthwhile to point out that the use of the above approach is based on two assumptions: (1) The apparent contact angle is a constant throughout the capillary rise process. (2) Soil specimens have similar qualities, that is, the variations of mineral constituents and solid structures (effective radius and number of capillary) in specimens are insignificant. This first assumption was tacitly approved by most CRM studies, while the second one can be satisfied by ensuring the similarities among soil specimens.

Two types of experiments were conducted in this study. For the first type, duplicate soil specimens made of the same soil were tested. All these specimens were prepared in the same way to ensure the similarity among them. The measured  $m-t$  curves were fitted using the fitting equations affiliated with different methods. In this way, the suitability of the above methods for analyzing the capillary rise in soils was tested. In the other type of experiment, the soils were sieved first to obtain soil groups of different average particle sizes. The purpose of this type of experiment is to investigate the variation of contact angle with respect to pore size.

**Table 2** Properties of test liquids

Test liquid	Density (kg/m <sup>3</sup> )	Surface tension (N/m)	Viscosity (N s/m <sup>2</sup> )
Pentane	626.2	$15.82 \times 10^{-3}$	$0.24 \times 10^{-3}$
Water	1,000	$71.79 \times 10^{-3}$	$1.002 \times 10^{-3}$

**Table 3** Properties of specimens made of soil A

Soil group	Sieve no.	Opening ( $\mu\text{m}$ )	Density <sup>a</sup> (g/cm <sup>3</sup> )	Content <sup>b</sup> (%)
1	20	840	1.10	16.21
2	40	420	1.06	19.69
3	50	300	1.02	13.38
4	60	250	0.98	5.38
5	70	210	0.98	6.92
6	80	180	0.96	6.89
7	120	125	0.94	7.77
8	140	105	0.88	7.44
9	170	90	0.73	8.02
10	200	75	0.77	8.49

<sup>a</sup> It is the dry density when the tube is fully packed by soil before vibration

<sup>b</sup> Content is the ratio of mass left on the sieve to the original total mass

### 3.2 Materials

For test liquids, water and pentane were used in this study, whose properties are listed in Table 2.

Two soils were used for both types of experiments: an Ohio subgrade soil (A) and a silica sand (B). Table 3 shows the soil group number, particle size, density of Soil A and the mass contents corresponding to different mesh sizes obtained in a sieve analysis. Table 4 provides similar information for Sand B. More than one specimen was

**Table 4** Properties of specimens made of Sand B

Soil group	Sieve no.	Opening ( $\mu\text{m}$ )	Density ( $\text{g}/\text{cm}^3$ )	Content (%)
1	20	840	1.43	60.02
2	40	420	1.38	20.76
3	50	300	1.35	5.19
4	60	250	1.31	7.27
5	70	210	1.30	3.35
6	80	180	1.23	1.69
7	120	125	1.23	1.74

Soil Group 8 includes all the soils passing Sieve 7

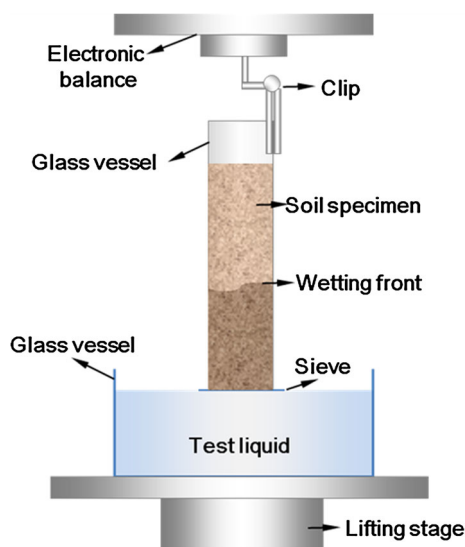


**Fig. 1** Instrument setup for CRM with Kruss 100 tensiometer

prepared and tested for each specimen number. So the densities listed in the tables are average values.

All soil specimens were prepared by strictly following the same procedure described below to ensure the similarity. A soil was poured into a tube at the same height as the top of the tube. The tube stood upright on a table. After the upper surface of the soil reached the top of the tube, the tube was vibrated with a small vibrator at a frequency of 55 Hz for 60 s. A metallic tool with a base and a vertically protruded pipe was used to accommodate the tube while it was on the vibrator. All vibrated soil specimens were then put into a tube rack for transportation and testing. A tissue roll and a piece of plastic wrap were used to protect the specimen from any further disturbance and pollution. The densities of the specimens in Tables 3 and 4 were used as important parameters for quality control.

### 3.3 Apparatus

A K100 Tensiometer, which is ‘a time-proven tool for making accurate surface and interfacial tension measurements’, was

used for the contact angle measurements [29]. Here we took advantage of its electronic balance instead of the built-in modules. As illustrated in Fig. 1, a self-fabricated tube filled with a soil was attached to the electronic balance with a clip. The rigid clip was used to reduce the time of self-stability for the electronic balance. A glass vessel with a test liquid in it was placed on a lifting stage below the tube. During a measurement, the lifting stage moved up until it got into contact with the sieve, which was glued at the bottom of the tube. The measurement of imbibed mass versus time was triggered when a contact was detected.

The glass tubes are 44.5 mm high and have an inner diameter of 5.75 mm and an outer diameter of 7.9 mm. The tubes were made of soda-lime glass in light of its comparatively high fracture toughness. The same number of metallic sieves with an opening of 75  $\mu\text{m}$  was prepared. These sieves were circular and had a diameter that was 1 mm bigger than the outer diameter of the tubes. Each sieve was glued to the bottom of a tube, which was sanded beforehand. The glue was chosen because of its high temperature resistance and chemical resistance. One of the great advantages of this design is that the influence of external meniscus is excluded [21]. As illustrated in Fig. 1, water is no more able to form an external meniscus due to the existence of the metallic sieve. Also, the errors caused by the thick glass sieves that used in previous studies were eliminated [22, 41].

### 3.4 Testing procedure

The following procedure was designed and strictly followed during the experiments.

1. All tubes and vessels were rinsed with acetone and then dried before tests.
2. The soils for test were dried in an oven (80 °C) for 24 h. Then the soil specimens of Soil A or Sand B were prepared by following the procedures described in Sect. 3.2. The specimens were covered with clean plastic wrap to avoid contamination.
3. Put the tube into the chamber of the tensiometer as illustrated in Fig. 1. And fill a rinsed vessel with test liquid according to the requirement of the tensiometer.
4. Close the chamber and start a test. Data were recorded immediately after the specimen gets into contact with the liquid. A measurement lasting a period of time ranging from 40 to 120 s. This time depends on soil types and was determined by trial tests.
5. Repeat Step 4 for another test. If a different test liquid is used, it is necessary to rinse the vessel with acetone.
6. After an experiment, all tubes were cleaned and dried. And data were collected for analysis.

Several issues require close attention during the process. First of all, clean gloves should be used throughout the

whole process to protect the specimens from being contaminated by the organic substance from hands. Secondly, aluminum foil was used under the bottom of the tubes to protect the sieves. Moreover, all the specimens were covered with plastic wrap to make sure the dry specimens would not be moisturized by the humidity in the air. Finally, further disturbances should be eliminated during the transport of the specimens.

It is worthwhile to point out the underlying assumptions for implementing CRM in the above ways. Firstly, the nature of the associated physical process, i.e., capillary rise, makes the proposed CRM more related to the wetting process and the advancing contact angle. Secondly, the curve fitting algorithms determines that a constant angle will be obtained. Considerations of the dynamic contact angle in capillary phenomena can be found in a few other studies [45, 52]. In addition, it should be noted that the experiments based on the above theoretical framework, whose results will be introduced in the following section, only covered a very short period of the capillary rise process. The major reasons are (1) the stages dominated by viscosity [20, 54], which mostly correspond to the first few seconds to several minutes, are enough for the purpose of the acquisition of contact angles; (2) measuring a much longer period using the current procedure may involve significant errors, such as the evaporation of the test liquid; and (3) the Lucas–Washburn equation alone may have difficulty in explaining phenomena in later stages such as capillary fingering [39]. However, significant efforts, such as [56] and [37], have been made in applying the Lucas–Washburn equation and its solutions to a time scale comparable with those in geotechnical applications, i.e., from minutes to years.

## 4 Results and discussions

### 4.1 Evaluation of traditional CRM (method 1)

The traditional CRM with the simplified Lucas–Washburn equation (Method 1) was performed first to evaluate its effectiveness and factors that could jeopardize its validity. Plotted in Fig. 2 are the measured  $m^2-t$  relationships for six specimens made of Soil A and Sand B. For each soil, two specimens were tested with pentane and another two tested with water. The initials in the legends denote the soils type (A or B); the following Arabic numbers represent the tube (specimen) number; and the last letters indicate the type of test liquid ('P' for pentane and 'W' for water). Comparisons between the results for specimens made of the same soil and measured with the same test liquid proved that the experiments have a good repeatability. As can be seen, the two relevant curves measured with pentane for both soils and those measured with water for Sand B almost coincide.

This indicates that the specimens prepared with the proposed procedures well ensured the similarities among specimens. However, a larger difference is found between the curves on the two specimens made of Soil A and measured with pentane. But this difference is acceptable considering the difficulties in ensuring the similarity between specimens. Even though, the shapes of the two curves are very similar except that specimen 6 has a greater initial value. The difference in the initial value could also be attributed to the unstable contact process.

A linear segment can be identified in some of the curves in Fig. 2. Such a linear segment corresponds to the phenomenon prescribed by Method 1, for which inertia and gravity are neglected. Most of the existing applications of the CRM in soils are based on the identification of the gradient of this linear range. As can be seen, all of the curves in Fig. 2a exhibit linearity after 10 s. While for Sand B, there are also evident linear segments in the curves measured with water between 2 and 5 s. However, it is difficult to identify a linear part in the curves measured with pentane for Sand B. Such a phenomenon that a linear segment does not always evidently exist has also been observed on the experimental results of other specimens. In other words, Method 1 is not always applicable, because the linearity predicted by the simplified Lucas–Washburn equation is difficult or even unable to be identified in some cases.

Moreover, a significant error could be produced by using Method 1 even an obvious linear segment could be identified. The main reason is that there is no criterion for locating the start and the end of this linear segment. Therefore, the subjectivity in determining the range of a linear segment for the subsequent linear regression could lead to an unexpected error. In order to investigate this effect, the derivatives of the  $m^2-t$  curves in Fig. 2 were calculated and illustrated in Fig. 3. Two curves appeared to have the best and worst linear parts for the two soils, respectively, were calculated. The derivatives are in fact the gradients of the curves, or more specifically, the values of parameter  $\kappa_1$  in the fitting equation of Method 1. As illustrated in Fig. 3a,  $\kappa_1$  for Soil A decreases to a level with respect to time. The value of  $\kappa_1$  predicted by Method 1 could be obtained by calculating the average gradient of a chosen linear segment. However, great oscillations in the data occur almost everywhere. The result measured with pentane is smoother than that with water. This agrees with the intuitive observation in Fig. 2a. It is observed that 120 points (around 3 s) were long enough to eliminate the oscillations by smoothing while short enough in comparison with the linear segment. So the smoothed curves were obtained by averaging every 120 neighboring points. The same method but with 40 neighboring points was adopted for smoothing data for Sand B in Fig. 3b. The smoothed

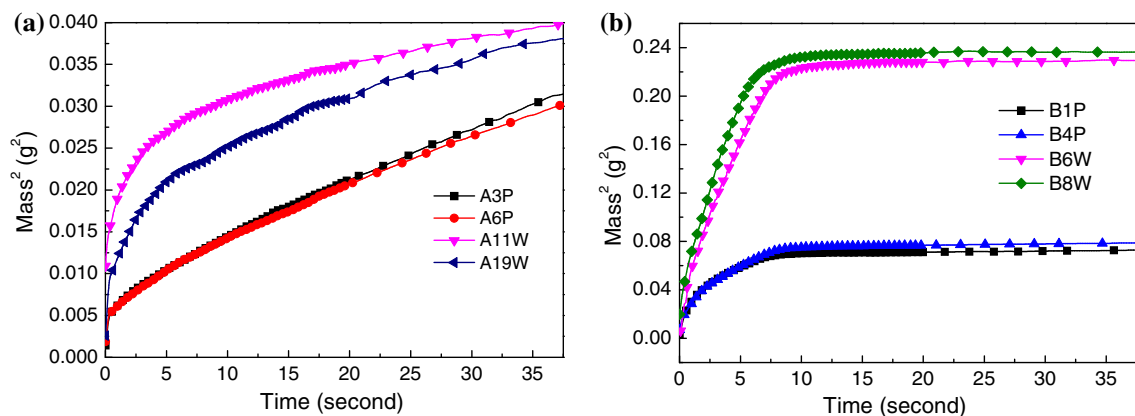


**Fig. 2** Measured  $m^2-t$  relationship for **a** Soil A; **b** Sand B

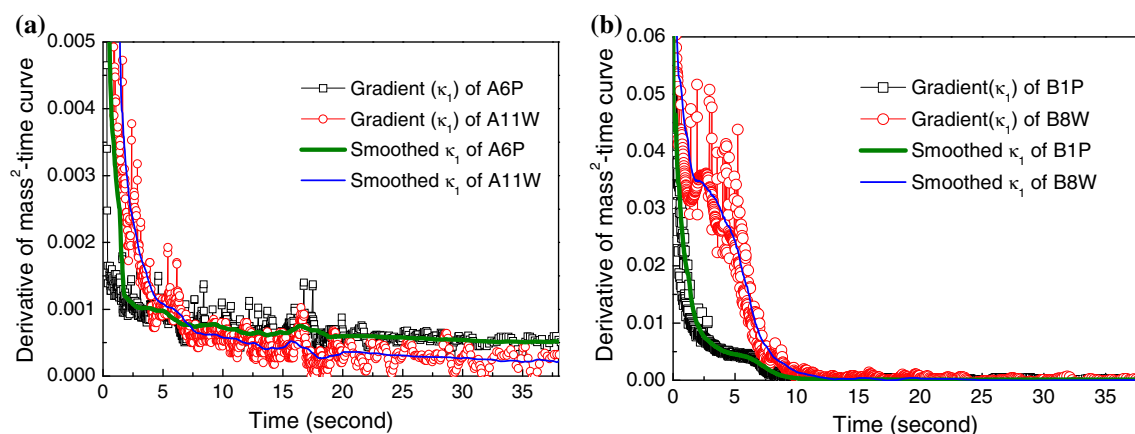


**Fig. 3** Gradient of measured  $m^2-t$  relationship ( $\kappa_1$ ) for **a** Soil A; **b** Sand B

curves show the change in linearity with respect to time. However, a significant difference in calculated values of  $\kappa_1$  could be expected if the data range for calculation is slightly changed.

In summary, a linear segment for calculating  $\kappa_1$  in Method 1 is difficult to be identified in some cases. Even when such a linear segment can be obviously observed in some measured  $m^2-t$  curves, the determination of its gradient could be very subjective. The accuracy is dependent on the choice of the start and end of the linear segment. Therefore, the rationality for Method 1, which is adopted by most of the existing CRM investigations, is jeopardized. Due to the reason, Method 1 was not included in the data analysis by means of curve fitting in the following study.

#### 4.2 A comparative study

To investigate the validity of Methods 2, 3 and 4 in analyzing the measured  $m-t$  curves for CRM, the corresponding fitted values of  $\kappa_2$ ,  $\kappa_3$  and  $\kappa_4$  obtained by using a nonlinear least squares curve fit were summarized in

**Table 5** Values of  $\kappa_j$  obtained by curve fitting for specimens made of unsieved Soil A

Specimen name	Method 2	Method 3	Method 4
A3P	$4.58 \times 10^{-4}$	$9.62 \times 10^{-1}$	$3.72 \times 10^{-4}$
A5P	$4.41 \times 10^{-4}$	$39.0 \times 10^{-1}$	$4.98 \times 10^{-4}$
A6P	$3.61 \times 10^{-4}$	5.94	$3.54 \times 10^{-4}$
A7P	$4.54 \times 10^{-4}$	1.06	$3.66 \times 10^{-4}$
A9P	$4.92 \times 10^{-4}$	0.33	$3.42 \times 10^{-5}$
A14W	$1.94 \times 10^{-4}$	$1.04 \times 10^{-1}$	$1.21 \times 10^{-4}$
A16W	$2.49 \times 10^{-4}$	$1.14 \times 10^{-1}$	$1.61 \times 10^{-4}$
A17W	$1.80 \times 10^{-4}$	$1.04 \times 10^{-1}$	$1.41 \times 10^{-4}$
A19W	$2.90 \times 10^{-4}$	$1.24 \times 10^{-1}$	$1.77 \times 10^{-4}$
A20W	$2.17 \times 10^{-4}$	$1.09 \times 10^{-1}$	$9.45 \times 10^{-5}$

Table 5 (for Soil A) and Table 6 (for Sand B). MATLAB code was developed to automate the data processing processes for the purpose of eliminating subjective factors.

The performances of the three fitting functions were evaluated by analyzing the results in Tables 5, 6, 7 and 8.

**Table 6** Values of  $\kappa_J$  obtained by curve fitting for specimens made of unsieved Sand B

Specimen name	Method 2	Method 3	Method 4
B1P	$5.88 \times 10^{-6}$	$2.23 \times 10^{-1}$	$7.63 \times 10^{-6}$
B2P	$2.36 \times 10^{-5}$	$1.92 \times 10^{-1}$	$8.75 \times 10^{-6}$
B3P	$3.02 \times 10^{-6}$	$2.11 \times 10^{-1}$	$9.64 \times 10^{-5}$
B4P	/	$2.23 \times 10^{-1}$	$7.38 \times 10^{-6}$
B5P	/	$2.10 \times 10^{-1}$	$2.92 \times 10^{-5}$
B6W	/	$4.83 \times 10^{-1}$	$1.04 \times 10^{-6}$
B7W	/	$4.80 \times 10^{-1}$	$7.37 \times 10^{-5}$
B8W	/	$4.60 \times 10^{-1}$	$1.01 \times 10^{-7}$
B9W	/	$4.64 \times 10^{-1}$	$1.71 \times 10^{-8}$
B10W	/	$4.54 \times 10^{-1}$	$1.34 \times 10^{-5}$

'/' means a value close to 0, i.e.,  $1 \times 10^{-12}$ , was obtained, which indicates that the curve fit failed

Firstly, we can see that Method 2 failed to give out a reasonable value for  $\kappa_J$  in many cases. And it turned out that most of these failures appeared in fitting the measured data for Sand B. This makes good sense because the fitting equation was derived from a governing equation without considering gravity, whose influence is significant as the height of capillary rise reaches a specific ratio (1/10) of equilibrium height [20] given by Eq. 22.

$$h_{\text{eq}} = \frac{2\gamma \cos(\tilde{\theta})}{\rho g \tilde{r}} \quad (22)$$

The experimental evidence that Method 2 was unable to provide a result in most cases indicates that gravity is an important factor for capillary rise in soils. And this factor needs to be considered when using the CRM for measuring the contact angle of soils. Fitting functions of Method 3 and Method 4 had a much better performance. Between them, Method 3 was effective in almost all conditions while Method 4 still failed in several cases. This comparison demonstrates that Method 3 has the best applicability within these three methods. Considering that Method 4 is a method that has been applied in physical chemistry, Method 3 should be a better and thus acceptable choice for CRM, at least with regard to the scope of application.

Secondly, the performance of the three methods can be compared by evaluating the repeatability in fitting the measured results from the first type of experiment. It is seen from Sect. 2.1 that the calculated value of the contact angle is dependent on the value of  $\kappa_J$  obtained by curve fitting. For the first type of measurement with unsieved soil specimens, close values of  $\kappa_J$  are expected since the specimens are similar to each other. The results listed in Tables 5 and 6 indicate that only the results obtained by Method 3 exhibited good repeatability for specimens made

**Table 7** Values of  $\kappa_J$  obtained by curve fitting for specimens made of sieved Soil A

Specimen name	Method 2	Method 3	Method 4
A1_1P	$9.37 \times 10^{-5}$	$2.01 \times 10^{-1}$	$1.27 \times 10^{-4}$
A1_2P	$7.14 \times 10^{-5}$	$9.32 \times 10^{-2}$	$5.22 \times 10^{-5}$
A1_3W	$1.31 \times 10^{-4}$	$2.84 \times 10^{-1}$	$3.79 \times 10^{-6}$
A1_4W	/	$3.28 \times 10^{-1}$	$2.40 \times 10^{-6}$
A2_5P	$1.31 \times 10^{-5}$	$2.72 \times 10^{-1}$	$8.98 \times 10^{-4}$
A2_6P	$1.86 \times 10^{-5}$	$2.78 \times 10^{-1}$	$1.00 \times 10^{-3}$
A2_7W	$1.26 \times 10^{-4}$	$2.11 \times 10^{-1}$	$6.39 \times 10^{-6}$
A2_8W	$1.82 \times 10^{-4}$	$2.18 \times 10^{-1}$	$1.02 \times 10^{-5}$
A3_9P	$4.13 \times 10^{-3}$	$4.40 \times 10^{-1}$	$3.09 \times 10^{-3}$
A3_10P	$4.20 \times 10^{-3}$	$4.78 \times 10^{-1}$	$3.73 \times 10^{-3}$
A3_11W	$7.21 \times 10^{-5}$	$4.34 \times 10^{-1}$	$6.24 \times 10^{-5}$
A3_12W	$2.81 \times 10^{-4}$	$1.33 \times 10^{-1}$	$8.44 \times 10^{-5}$
A4_13P	/	$3.71 \times 10^{-1}$	/
A4_14P	/	$4.90 \times 10^{-1}$	/
A4_15W	$2.41 \times 10^{-4}$	$1.84 \times 10^{-1}$	$2.02 \times 10^{-4}$
A4_16W	$2.25 \times 10^{-4}$	1.16	$2.01 \times 10^{-4}$
A5_17P	/	$4.52 \times 10^{-1}$	$2.70 \times 10^{-4}$
A5_18P	/	1.27	$1.93 \times 10^{-3}$
A5_19W	$4.61 \times 10^{-4}$	$2.44 \times 10^{-1}$	$2.60 \times 10^{-4}$
A5_20W	$2.37 \times 10^{-4}$	$2.06 \times 10^{-1}$	$2.20 \times 10^{-4}$
A6_1P	$1.14 \times 10^{-3}$	99.14	/
A6_2P	$7.26 \times 10^{-4}$	80.69	$5.02 \times 10^{-4}$
A6_3W	/	/	/
A6_4W	$2.00 \times 10^{-4}$	$9.15 \times 10^{-2}$	$1.16 \times 10^{-4}$
A7_5P	$3.04 \times 10^{-4}$	57.15	$2.99 \times 10^{-4}$
A7_6P	$4.31 \times 10^{-4}$	40.31	$2.40 \times 10^{-4}$
A7_7W	$1.86 \times 10^{-4}$	$1.08 \times 10^{-1}$	$1.26 \times 10^{-4}$
A7_8W	$6.34 \times 10^{-5}$	$6.18 \times 10^{-2}$	$5.61 \times 10^{-5}$
A8_9P	$3.33 \times 10^{-4}$	52.47	$3.28 \times 10^{-4}$
A8_10P	$5.17 \times 10^{-4}$	61.58	$3.73 \times 10^{-4}$
A8_11W	$7.68 \times 10^{-5}$	$6.56 \times 10^{-2}$	$5.06 \times 10^{-5}$
A8_12W	$8.51 \times 10^{-5}$	$5.42 \times 10^{-2}$	$4.55 \times 10^{-5}$
A9_13P	$5.87 \times 10^{-4}$	78.61	$4.91 \times 10^{-4}$
A9_14P	$4.27 \times 10^{-4}$	68.72	$4.18 \times 10^{-4}$
A9_15W	$9.00 \times 10^{-5}$	/	$8.79 \times 10^{-5}$
A9_16W	$2.11 \times 10^{-4}$	$6.03 \times 10^{-2}$	$4.59 \times 10^{-5}$
A10_17P	$4.14 \times 10^{-4}$	64.05	$4.11 \times 10^{-4}$
A10_18P	$5.97 \times 10^{-4}$	73.71	$5.23 \times 10^{-4}$
A10_19W	$1.28 \times 10^{-4}$	$6.43 \times 10^{-2}$	$4.62 \times 10^{-5}$
A10_20W	$1.19 \times 10^{-4}$	$7.12 \times 10^{-2}$	$3.09 \times 10^{-5}$

In the specimen name, the Arabic number in front of the hyphen is the soil group number and that after the hyphen is the tube number (all tubes used were numbered)

of both Soil A and Sand B. The obtained values of  $\kappa_3$  for the specimens measured with the same test liquid are very close to each other. Considering the variations in effective radius and tortuosity, the results are very encouraging. And

**Table 8** Values of  $\kappa_j$  obtained by curve fitting for specimens made of sieved Sand B

Specimen name	Method 2	Method 3	Method 4
B1_1P	$7.04 \times 10^{-5}$	$1.64 \times 10^{-1}$	$4.05 \times 10^{-6}$
B1_1P <sup>a</sup>	$4.68 \times 10^{-4}$	$1.73 \times 10^{-1}$	$4.35 \times 10^{-6}$
B1_2W	/	1.54	$1.07 \times 10^{-2}$
B1_2W <sup>a</sup>	/	$5.82 \times 10^{-1}$	$1.28 \times 10^{-5}$
B2_3P	$1.49 \times 10^{-4}$	$2.08 \times 10^{-1}$	$1.14 \times 10^{-4}$
B2_3P <sup>a</sup>	/	$2.29 \times 10^{-1}$	$4.97 \times 10^{-5}$
B2_4W	/	$5.93 \times 10^{-1}$	$5.63 \times 10^{-7}$
B2_4W <sup>a</sup>	/	$5.72 \times 10^{-1}$	$6.27 \times 10^{-7}$
B3_5P	/	$3.27 \times 10^{-1}$	$2.38 \times 10^{-6}$
B3_5P <sup>a</sup>	/	$3.05 \times 10^{-1}$	$4.26 \times 10^{-6}$
B3_6W	/	$6.19 \times 10^{-1}$	$9.36 \times 10^{-2}$
B3_6W <sup>a</sup>	/	$5.87 \times 10^{-1}$	/
B4_7P	/	$3.13 \times 10^{-1}$	$3.01 \times 10^{-6}$
B4_7P <sup>a</sup>	/	$3.37 \times 10^{-1}$	$2.01 \times 10^{-6}$
B4_8W	/	$6.88 \times 10^{-1}$	/
B4_8W <sup>a</sup>	/	$6.12 \times 10^{-1}$	/
B5_9P	/	$3.22 \times 10^{-1}$	$1.02 \times 10^{-7}$
B5_9P <sup>a</sup>	/	$3.17 \times 10^{-1}$	$3.50 \times 10^{-6}$
B5_10W	/	$8.14 \times 10^{-1}$	$3.77 \times 10^{-3}$
B5_10W <sup>a</sup>	/	$6.24 \times 10^{-1}$	/
B6_11P	/	$3.51 \times 10^{-1}$	$1.01 \times 10^{-7}$
B6_11P <sup>a</sup>	/	$3.20 \times 10^{-1}$	$1.20 \times 10^{-6}$
B6_12W	/	$9.00 \times 10^{-1}$	$2.82 \times 10^{-3}$
B6_12W <sup>a</sup>	/	$6.94 \times 10^{-1}$	/
B7_13P	/	$3.34 \times 10^{-1}$	/
B7_13P <sup>a</sup>	/	$3.43 \times 10^{-1}$	$1.07 \times 10^{-6}$
B7_14W	/	1.10	$5.69 \times 10^{-3}$
B7_14W <sup>a</sup>	/	$6.15 \times 10^{-1}$	/
B8_15P	/	$3.82 \times 10^{-1}$	$1.31 \times 10^{-6}$
B8_15P <sup>a</sup>	/	$3.59 \times 10^{-1}$	$6.18 \times 10^{-5}$
B8_16W	/	1.55	$1.07 \times 10^{-2}$
B8_16W <sup>a</sup>	/	$6.48 \times 10^{-1}$	/

<sup>a</sup> The result was measured with the same sieved soil, same tube, and same test liquid but different specimens

a large absolute value of the difference between  $\kappa_j$ 's measured on different specimens does not mean a great difference is the measured contact angles because the arccosine function will be used. Method 2 obtained comparative good results for the specimens made of Soil A, but bad results for that made of Sand B. This is due to the reason described in the last paragraph. It is thus concluded that Method 2 is appropriate for CRM only if the range of capillary rise is restrained to the very first stage of water imbibitions, when the water front is far from equilibrium height. Results obtained by Method 4 show comparatively significant differences among specimens tested with the same liquid. The results are thus far from satisfactory.

The performance of the three methods can also be evaluated by identifying the trends in the change of  $\kappa_j$  measured with different methods. It is reasonable to anticipate that  $\kappa_j$  changes in a specific pattern, or at least change in a consecutive way with respect to mesh size. As listed in Tables 7 and 8, results indicate that Method 3 yielded some trends in the change of  $\kappa_3$  while the other two methods did not. In Table 7, the trend in the variations of fitted value of  $\kappa_3$  in Sand B specimens is evident: it increases as particle size decreases for both pentane and water. For specimens made of Soil A in Table 7,  $\kappa_3$  increases as particle size decreases for the specimens tested with pentane while  $\kappa_3$  decreases as particle size decreases for that with water. However, this trend is not as evident as the one in the results for Sand B specimens. A possible reason for the less evident trend in the results for Sand A specimens is that its constituents could change with respect to particle radius since it is a subgrade soil while Sand B is a commercial product composes 99.7 % silicon dioxide.

Based on the discussion on the fitting results, it is now safe to conclude that Method 3 is the most appropriate for the contact angle measurement based on the dynamics of the capillary rise. The method yielded reasonable results for almost all specimens tested. And the results obtained by applying the fitting function derived by the method exhibited good repeatability for the specimens made of the same soil and also tested with the same liquid. Moreover, good continuities were found in the fitted results as the radii of specimens change and some specific patterns have been identified accordingly. Typical comparisons between measured and fitted  $m-t$  curves are illustrated in Figs. 4 and 5. As can be seen, the fitted results match very well with measured data. As illustrated in Fig. 4, the measured and fitted curves almost coincide. This in turn proved that the solution to the governing equation proposed by Method 3 well describes the dynamics of capillary rise in these Soil A specimens. For Sand B, it is noticed that the match between measured and fitted results are not as good as that for Soil A specimens but is still acceptable. Two possible reasons for these differences were identified: (1) the process of capillary rise is much faster in Sand B specimens than that in Soil A specimens, which could lead to more uncertainties and make the measured curves deviate from that predicted under ideal conditions; (2) the influence of inertia is relatively significant in the Sand B specimens yet not considered by the governing equation. The average apparent contact angle for the unsieved Soil A specimens and unsieved Sand B specimens are  $89.43^\circ$  and  $60.93^\circ$  by Method 3.

#### 4.3 Conditions for applying method 3

As discussed above, one of the main reasons for errors in applications of Method 3 is the overlook of the influence of

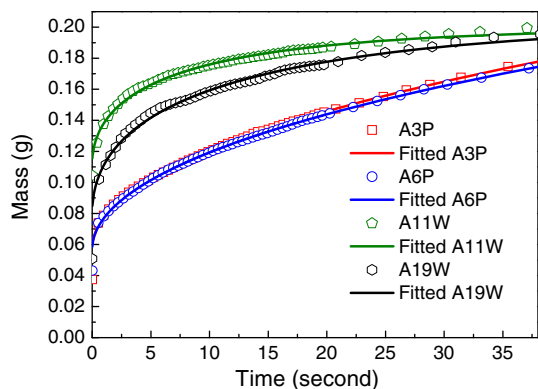


Fig. 4 Measured and fitted  $m-t$  curve for unsieved Soil A specimens

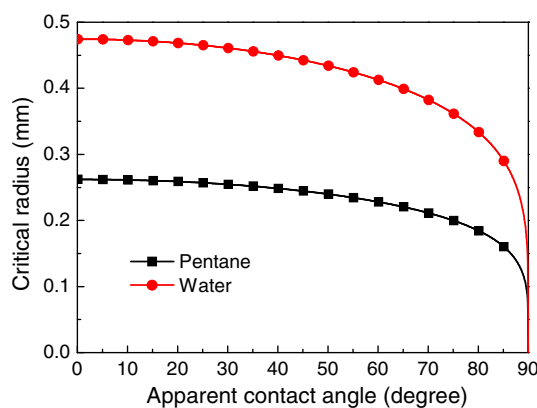


Fig. 6 Critical radius for the influence of inertia

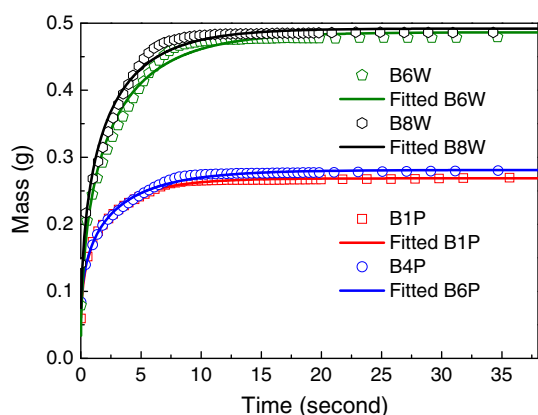


Fig. 5 Measured and fitted  $m-t$  curve for unsieved Sand B specimens

inertial force. And this influence may be significant in the very beginning of a capillary rise. It was reported that the influence of inertia is insignificant whenever  $r$  (or effective radius in porous media) is smaller than a critical radius,  $r_c$ , which satisfies the following relation [27]:

$$r_c = 2 \frac{(\gamma \cos(\theta) \eta^2 \rho^2 g^3)^{1/5}}{\rho g} \tag{23}$$

This relation can be illustrated schematically by Fig. 6.

On the other hand, the effective radius can be calculated by Eq. 24.

$$\tilde{r} = \left( \frac{16 \alpha_3 \gamma_p \eta_p}{\rho_p^2 g^2} \right)^{1/3} \tag{24}$$

where  $\alpha_3$  is the constant for curve fitting in Table 1 by using the measured curve tested with pentane. The average effective radii for the specimens made of Soil A and Sand B are  $8.51 \times 10^{-3}$  and  $7.23 \times 10^{-2}$  mm, respectively. From Fig. 6 we can see that both of the radii are much

smaller than the critical radius as long as the apparent contact angle is smaller than  $89.9^\circ$ . For the hydrophilic soils affiliated with SWCCs, the contact angle is usually much smaller than this value. So it is safe to apply Method 3 as long as the soil tested is not course-grained soils with an approximately neutral wettability (at a contact angle of  $90^\circ$ ). Based on this comparative study, Method 3 is suggested as a modified CRM to take the place of the conventional CRM based on the simplified Lucas–Washburn equation (Method 1).

#### 4.4 A unique feature of the contact angle of porous materials

The original definition of the contact angle is the angle conventionally measured through the liquid, where a liquid/vapor interface meets a solid surface. This angle, which quantifies the wettability of a solid surface by a liquid via the Young equation, is frequently referred to as intrinsic contact angle in some literature. However, the perfectly smooth solid surface in the definition of intrinsic contact angle does not exist in porous materials. Instead, a bundle of capillaries with different pore radii and irregular shaped pore surfaces exist. Also, different constituents may be distributed diversely at different scales. It was therefore estimated that the contact angle of porous materials is influenced by some factors, such as the average pore size. This could be a feature only belonging to porous materials. This thought is one of the major reasons to conduct the second type of experiment.

The variations of contact angle with respect to the aggregate size for Soil A and Sand B are illustrated in Figs. 7 and 8, respectively. The radii were calculated with the opening sizes in the sieve analyses. The contact angle is an average value and corresponds to the group of soil that passing through the sieve of corresponding opening size.

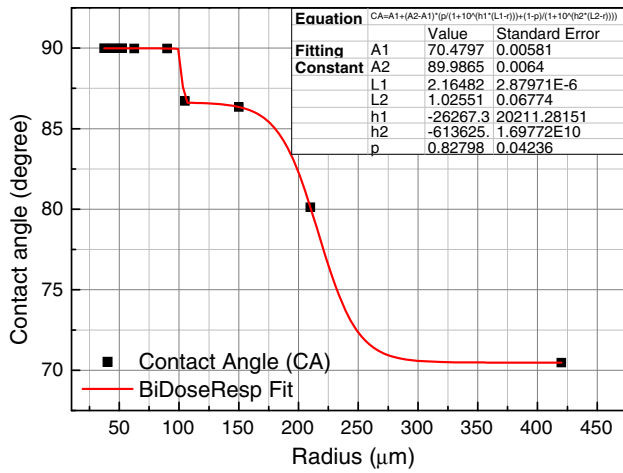


Fig. 7 Contact angle versus sieve opening (Soil A)

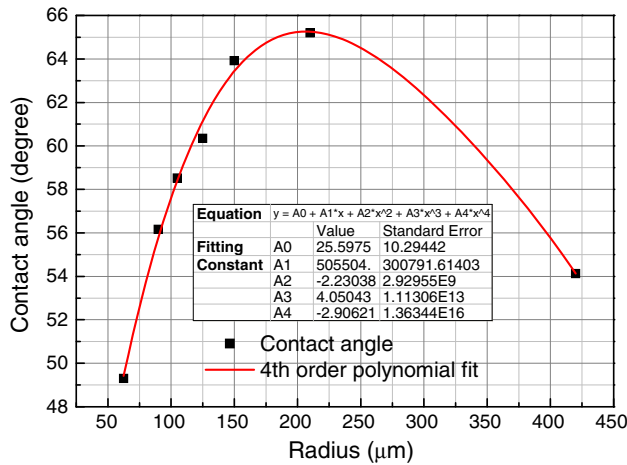


Fig. 8 Contact angle versus sieve opening (Sand B)

The trends observed in the fitting constants in the comparative study now manifest themselves in the variations of contact angles with respect to aggregate size. For Soil A, it is clear that the contact angle increases as aggregate size decreases; while for Sand B, contact angle increases at first and then decreases as aggregate size decreases. Two main factors were identified to be responsible for the variations of the contact angle versus aggregate size: organic matter content and roughness. These two factors were also believed to be the reason for the different trends in Soil A and Sand B. Soil A is a subgrade soil obtained directly from a construction site, it is natural and possibly contains a considerable content of organic matter. These organic materials could reduce the wettability of the soil significantly. In addition, these organic materials are easier to accumulate in smaller pores of greater specific surface area and thus more significantly reduce the wettability of soil specimens of smaller effective diameters [16, 44]. The

variation of contact angle versus particle size in Sand B may be in the charge of another factor, that is, roughness, since the organic matter content is relatively low. The impact of surface roughness on contact angle is given by the Wenzel equation as follows [50]:

$$\cos \theta = \zeta \cos \theta_s \tag{25}$$

where  $\zeta$  is the roughness ratio and  $\theta_s$  is the contact angle for the smooth surface. The roughness factor,  $\zeta$ , is the ratio between the actual surface area and the apparent surface area of a rough surface [60]. This equation predicts that, for hydrophilic soils, a higher roughness ratio leads to a smaller contact angle. That is, increasing roughness will contribute to an increase in wettability in hydrophilic soils [15, 55]. Additionally, the roughness of the equivalent cylindrical capillaries of smaller pores is more sensitive to particle surface morphology, which results in a higher equivalent roughness in smaller pores. The influence of this factor prevails over the effect of the relatively small amount of organic matter when the particle size is small enough. This is possibly the reason why the contact angle decreases as the particle size decreases after an initial increase with the decrease of particle size in the larger particle size range.

### 5 Conclusion

This paper reports a comprehensive study on the application of the capillary rise method in measuring the contact angles of porous materials. The general background for the CRM was reviewed, and more theoretical treatments for a modified CRM method were presented. The disadvantages of the traditional CRM investigations were demonstrated with experiments. By employing a comparative study, a modified CRM (Method 3) was proposed based on the analytical solution to one form of the Lucas–Washburn equation. This modified CRM exhibits a reliable performance on numerous unsieved and sieved (different average particle sizes) samples made of a subgrade soil and a silicon dioxide sand. Designed specimen preparation and testing procedures together with self-fabricated apparatuses for the specimen preparation, transport, and accommodation were introduced. For the two types of experiments conducted with the modified CRM, experimental results for unsieved specimens showed good repeatability, while clear trends in the variations of the contact angle with respect to the particle size were observed in the experimental results for the two different types of sieved soils. Contact angles much greater than zero were observed for all of the tested specimens. This result contradicts the assumption of perfect wettability in many existing SWCC studies. While it was qualitatively observed in the past that soil does not

always behave perfect wetting except during drying process, this study provides direct quantitative experimental data to confirm that perfect wetting may not exist in wetting processes.

This preliminary study aimed at presenting a pioneering study in geotechnical engineering to study the interactions between phases in terms of contact angle. The CRM may be further developed by curve fitting using the complete Lucas–Washburn equation directly, in which inertia is considered and no analytical solution is necessary. Several issues of CRM, such as the assumption of a constant contact angle, throughout a capillary rise process need to be further validated. More CRM tests on different types of soils will be very beneficial, and a data base for contact angles of different soils in engineering is extremely helpful. Several factors affecting the contact angle of soils, such as particle size, constituents, saturation, temperature, and hysteresis need further investigations.

**Acknowledgments** The authors acknowledge Dr. Adin Mann in the Department of Chemical Engineering at Case Western Reserve University for the inspiring discussions on contact angle measurements with the CRM and the access to the surface engineering instruments. We also thank Dr. Vladimir Gurau for the laboratory orientation and for sharing MATLAB code for data processing.

## References

1. Abu-Zreig M, Rudra RP, Dickinson WT (2003) Effect of application of surfactants on hydraulic properties of soils. *Biosyst Eng* 84(3):363–372
2. Adamson AW (1990) *Physical chemistry of surfaces*, 5th edn. Wiley, New York
3. Anderson MA, Hung AYC, Mills D, Scott MS (1995) Factors affecting the surface tension of soil solutions and solutions of humic acids. *Soil Sci* 160:111–116
4. Arya LM, Paris JF (1981) A physicoempirical model to predict soil moisture characteristics from particle-size distribution and bulk density data. *Soil Sci Soc Am J* 45:1023–1030
5. Bachmann J, van der Ploeg RR (2002) A review on recent developments in soil water retention theory: interfacial tension and temperature effects. *J Plant Nutr Soil Sci* 165(4):468–478
6. Bachmann J, Horton R, van der Ploeg RR, Woche SK (2000) Modified sessile drop method for assessing initial soil–water contact angle of sandy soil. *Soil Sci Soc Am J* 64:564–567
7. Bachmann J, Woche SK, Goebel M-O, Kirkham MB, Horton R (2004) Extended methodology for determining wetting properties of porous media. *Water Resour Res* 39(12):1353
8. Barry DA, Parlange J-Y, Li L, Prommer H, Cunningham CJ, Stagnitti F (2000) Analytical approximations for real values of the Lambert W-function. *Math Comput Simul* 53:95–103
9. Bikerman JJ (1950) Surface roughness and contact angle. *J Phys Chem* 54:653–658
10. Czachor H (2006) Modelling the effect of pore structure and wetting angles on capillary rise in soils having different wettabilities. *J Hydrol* 328:604–613
11. Czachor H (2007) Applicability of the Washburn theory for determining the wetting angle of soils. *Hydrol Process* 21(17):2239–2247
12. De Jonge LW, Jacobsen OH, Moldrup P (1999) Soil water repellency: effects of water content, temperature, and particle size. *Soil Sci Soc Am J* 63:437–442
13. Dekker LW, Ritsema CJ (2000) Wetting patterns and moisture variability in water repellent Dutch soils. *J Hydrol* 231:148–164
14. Doerr SH, Shakesby RA, Walsh RPD (2000) Soil water repellency: its causes, characteristics and hydro-geomorphological significance. *Earth Sci Rev* 51:33–65
15. Drelich J, Miller JD (1994) The effect of solid surface heterogeneity and roughness on the contact angle/drop (bubble) size relationship. *J Colloid Interface Sci* 164:252–259
16. Ducarior J, Lamy I (1995) Evidence of trace metal association with soil organic matter using particle size fractionation after physical dispersion treatment. *Analyst* 120:741–745
17. Dullien FAL, El-Sayed MS, Batra VK (1977) Rate of capillary rise in porous media with nonuniform pores. *J Colloid Sci* 60:497–506
18. Fredlund DG, Xing A (1994) Equations for the soil-water characteristic curve. *Can Geotech J* 31(4):521–532. doi:10.1139/t94-061
19. Fries N, Dreyer M (2008) An analytic solution of capillary rise restrained by gravity. *J Colloid Interface Sci* 320:259–263
20. Fries N, Dreyer M (2008) The transition from inertial to viscous flow in capillary rise. *J Colloid Interface Sci* 327:125–128
21. Friess BR, Hoorfar M (2010) Measurement of internal wettability of gas diffusion porous media of proton exchange membrane fuel cells. *J Power Sources* 195:4736–4742
22. Geobel M-O, Bachmann J, Woche SK, Fischer WR, Horton R (2004) Water potential and aggregate size effects on contact angle and surface energy. *Soil Sci Soc Am J* 68:383–393
23. Grant SA, Bachmann J (2002) Effect of temperature on capillary pressure. *Geophys Monogr* 129:199–212
24. Grant SA, Salehzadeh A (1996) Calculation of temperature effects on wetting coefficients of porous solids and their capillary pressure functions. *Water Resour Res* 32(2):261–270
25. Grundke K (2002) Wetting, spreading and penetration. In: Holmberg K (ed) *Handbook of applied surface and colloid chemistry*. Wiley, London
26. Gurau V, Mann JA (2010) Technique for characterization of the wettability properties of gas diffusion media for proton exchange membrane fuel cells. *J Colloid Interface Sci* 350(2):577–580
27. Hamraoui A, Nylander T (2002) Analytical approach for the Lucas–Washburn equation. *J Colloid Interface Sci* 250:415–421
28. King PM (1981) Comparison of methods for measuring severity of water repellence of sandy soils and assessment of some factors that affect its measurement. *Aust J Soil Res* 19:275–285
29. Kruss Tensiometer 100 Instruction Manual V020715, Kruss GmbH, Hamburg, 2001
30. Kubiak KJ, Wilson MCT, Mathia TG, Carval PH (2010) Wettability versus roughness of engineering surfaces. *Wear* 271(3–4):523–528
31. Letey J (1969) Measurement of contact angle, water drop penetration time, and critical surface tension. In: DeBano LF, Letey J (eds) *Proceedings of symposium on water-repellent soils*. University of California, Riverside, pp 43–47
32. Letey J, Osborn J, Pelishek RE (1962) Measurement of liquid solid contact angles in soil and sand. *Soil Sci* 93:149–153
33. Levine S, Lowndes J, Watson EJ, Neale G (1980) A theory of capillary rise of a liquid in a vertical cylindrical tube and in a parallel-plate channel Washburn equation modified to account for the meniscus with slippage at the contact line. *J Colloid Interface Sci* 73(1):136–151
34. Likos WJ, Lu N (2004) Hysteresis of capillary stress in unsaturated granular soil. *J Eng Mech* 130(6):646–655
35. Liu Z, Yu X, Wan L (2013) Influence of contact angle on soil–water characteristic curve with modified capillary rise method. *Transp Res Rec J Transp Res Board* 2349(1):32–40

36. Lu N, Likos WJ (2004) *Unsaturated soil mechanics*. Wiley, New York
37. Lu N, Likos WJ (2004) Rate of capillary rise. *J Geotech Geoenviron Eng* 130:464
38. Lucas R (1918) Rate of capillary ascension of liquids. *Kolloid Z* 23:15
39. Medici E, Allen J (2011) Scaling percolation in thin porous layers. *Phys Fluids* 23(12):122107
40. McGhie DA, Posner AM (1980) Water repellence of a heavy-textured Western Australian surface soil. *Aust J Soil Res* 18:309–323
41. Michel J-C, Riviere L-M, Bellon-Fontaine M-N (2001) Measurement of the wettability of organic materials in relation to water content by the capillary rise method. *Eur J Soil Sci* 52:459–467
42. Morrow NR (1970) Physics and thermodynamics of capillary. *Ind Eng Chem* 62(6):32–56
43. Niggemann J (1970) Versuche zur Messung der Benetzungsfähigkeit von Torf. *Torfnachrichten* 20:14–18
44. Oades JM (1988) The retention of organic matter in soils. *Biogeochemistry* 5(1):35–70
45. Popescu MN, Ralston J, Sedev R (2008) Capillary rise with velocity-dependent dynamic contact angle. *Langmuir* 24:12710–12716
46. Quere D (2008) Wetting and roughness. *Annu Rev Mater Res* 38:71–99
47. Ramirez-Flores J, Woche SK, Bachmann J, Goebel M-O, Hallett PD (2008) Comparing capillary rise contact angles of soil aggregates and homogenized soil. *Geoderma* 146:336–343
48. Ramon-Torregrosa PJ, Rodriguez-Valverde MA, Amirfazli A, Cabrerizo-Vilchez MA (2008) Factors affecting the measurement of roughness factor of surfaces and its implications for wetting studies. *Colloids Surf A Physicochem Eng Asp* 323:83–93
49. Reeker R (1954) Die Benetzungsfähigkeit von Torfmull. *Torfnachrichten* 7:15–16
50. Ryan BJ, Poduska KM (2008) Roughness effects on contact angle measurements. *Am J Phys* 76(11):1074–1077
51. Schoelkopf J, Gane PAC, Ridgway CJ, Matthews CP (2002) Practical observation of deviation from Lucas–Washburn scaling in porous media. *Colloids Surf A Physicochem Eng Asp* 206(1–3):445–454
52. Siebold A, Nardin M, Schultz J, Walliser A, Oppliger M (2000) Effect of dynamic contact angle on capillary rise phenomena. *Colloids Surf A* 161:81–87
53. Siebold A, Walliser A, Nardin M, Oppliger M, Schultz J (1997) Capillary rise for thermodynamic characterization of solid particle surface. *J Colloid Interface Sci* 186:60–70
54. Stange M, Dreyer ME, Rath HJ (2003) Capillary driven flow in circular cylindrical tubes. *Phys Fluids* 15(9):2587–2601
55. Tamai Y, Aratani K (1972) Experimental study of the relation between contact angle and surface roughness. *J Phys Chem* 76(22):3267–3271
56. Terzaghi K (1943) *Theoretical soil mechanics*. Wiley, New York
57. Tuller M, Or D, Dudley LM (1999) Adsorption and capillary condensation in porous media: liquid retention and interfacial configurations in angular pores. *Water Resour Res* 35(7):1949–1964
58. Vorvort RW, Cattle SR (2003) Linking hydraulic conductivity and tortuosity parameters to pore space geometry and pore-size distribution. *J Hydrol* 272:36–49
59. Washburn EW (1921) The dynamics of capillary flow. *Phys Rev* XVII 3:273–283
60. Wenzel RN (1936) Resistance of solid surfaces to wetting by water. *Ind Eng Chem* 28(8):988–994
61. Xue HT, Fang ZN, Yang Y, Huang JP, Zhou LW (2006) Contact angle determined by spontaneous dynamic capillary rises with hydrostatic effects: experiment and theory. *Chem Phys Lett* 432:326–330
62. Zhmud BV, Tiberg F, Hallstenson K (2000) Dynamics of capillary rise. *J Colloid Interface Sci* 22(8):263–269